GEOL 1008 1995

Pergamon

*Journal of Structural Geology*, Vol. 17, No. 12, pp. 1725 to 1740, 1995

0191-8141/95 $9.50+0.00

0191-8141(95)00066-6

# Compressional and extensional tectonics in an arc system: example of the Southern Apennines

J.-C. HIPPOLYTE, J. ANGELIER and E. BARRIER

Département de Géotectonique (URA 1759 du CNRS), Université P. et M. Curie, Boîte 129, 75252 Paris Cedex 05, France

(*Received* 28 *October* 1994; *accepted in revised form* 1 *June* 1995)

**Abstract**—Adopting the Southern Apennines as a case example, we determine the relationships between extensional and compressional structures within an arc system, based on tectonic analysis in the field. We show that, in addition to the well-known occurrence of inner extensional structures during frontal accretion, two other types of extensional structures are present in the Southern Apennines. We classify the three types of extensional structures depending on their chronologies with the accretion of the thrust unit, and we characterize them in terms of palaeostresses.

Some normal faults of the mountain chain are old extensional structures formed in a foreland basin. In the Matese Mountains, such faults with offsets ranging several hundred metres are sealed by a late Neogene thrust sheet. These foredeep structures were created by extension trending almost perpendicular to the axis of the present-day foreland basin.

Other normal faults, located closer to the Tyrrhenian sea, developed simultaneously with the Pliocene–Quaternary accretion of thrust sheets at the front of the belt. In the Salerne graben (a Tyrrhenian Basin structure), extension occurred perpendicular to the compression that prevailed at the front of the mountain belt. A stress gradient existed between the outer part of the arc (with $\sigma_1$ trending ENE–WSW) and the inner part (with $\sigma_2$ trending ENE–WSW).

In the Southern Apennines, middle Pleistocene–Holocene normal faults post-date all compression and thrusting. The corresponding recent stress field (NE–SW extension) results from uplift of the previously subsiding Adriatic lithosphere.

We conclude that a given thrust unit of this NW–SE-trending mountain chain may have successively undergone NE–SW extension in the foreland basin, NE–SW compression during the accretion, NW–SE extension in the back-arc region and NE–SW extension during the recent evolution of the prism. The succession of these tectonic regimes has induced complex structures, as commonly observed in an arc system.

## INTRODUCTION

Understanding the mechanism that allows co-existence of compression in an accretionary prism and extension in a back-arc basin is a major issue in the study of arc systems. In the Western Mediterranean, the Tyrrhenian arc (Apennines, Calabria and Sicilia) and its back-arc basin (Fig. 1a) show the juxtaposition of these two distinct modes of deformation. Extensional and compressional tectonics were active during the same period, simultaneous with the Neogene rollback of the sinking Ionian lithosphere (Moussat 1983, Malinverno & Ryan 1986). Most of the Apennines mountain belt results from late Miocene–Quaternary compression (Casero *et al.* 1988, Patacca *et al.* 1990). At the same time, extension produced the Tyrrhenian oceanic Basin partly superimposed on the eo-Alpine chain (Haccard *et al.* 1972, Scandone 1979). The Tyrrhenian Basin is in a back-arc position with respect to the late Miocene–Quaternary chain. It is composed of two sub-basins (Fig. 1a): the Vavilov sub-basin opened in the western part of the present Tyrrhenian sea during late Miocene and Pliocene, whereas, to the southeast, the Marsili sub-basin opened during Pliocene–Quaternary (Finetti & Del Ben 1986, Sartori 1989, Kasten *et al.* 1990).

Structural analyses onshore in the Tyrrhenian arc allow determination of the relationships between these two contrasting tectonic processes. It was shown that compressional and extensional structures (Fig. 1b) are superimposed in various ways. However, their genetic relationships are often obscure. Since most extensional structures post-date compression (e.g. Boccaletti *et al.* 1983), the presence of extension in the mountain chain is usually interpreted as the result of the eastward migration of the Tyrrhenian extensional area (e.g. Boccaletti *et al.* 1983, Malinverno & Ryan 1986, Bartole *et al.* 1984, Doglioni 1991, Fusi & Garduno 1992, Oldow *et al.* 1993). On the other hand, inversion of extensional structures may be related to block rotations (Knott & Turco 1991). More complex chronological relationships between extensional and compressional structures may also result from alternating periods of compression and extension in the same area (e.g. Gars 1983, Auroux 1984, Boccaletti *et al.* 1984, Bernini *et al.* 1990).

In this paper, we address the problem of space and time distribution of tectonic forces in terms of stresses. Our approach is based on measurements of fault slip orientations. We use the stress inversion techniques (Angelier 1989) to relate the observed structures to their causative tectonic forces. Favourable conditions for such a study were found in the Southern Apennines (Fig. 1b). The chronology of structures and stresses is established based on successions of tectonic movements and

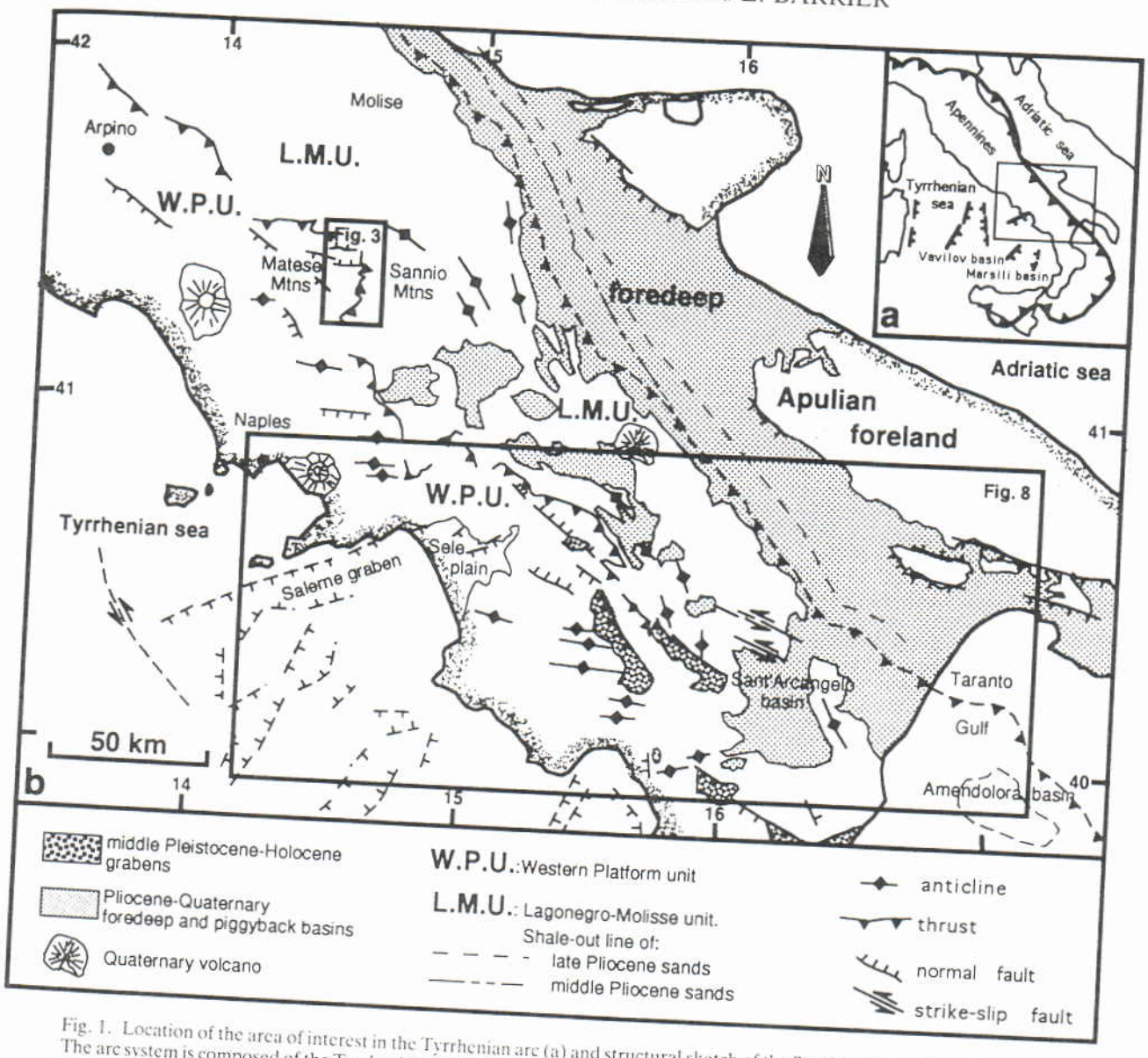


Fig. 1. Location of the area of interest in the Tyrrhenian arc (a) and structural sketch of the Southern Apennines, Italy (b). The arc system is composed of the Tyrrhenian arc, its foreland basin and its back-arc basin including the Vavilov and Marsili sub-basins. Note in (b) the mixture of compressional and extensional structures in the mountain belt. The shale-out lines, from Casero *et al.* (1991) show the progressive foredeep sediments onlap on the carbonates of the Apulian foreland, as well as the major advance of the thrust front in the southern area. The frontal thrust is buried under middle Pleistocene–Recent sediments.

stratigraphic dating, including the identification of syntectonic marine sediments of various ages. Combined palaeostress determinations and structural analyses enable us to determine the age, origin and significance in the history of the arc of the observed extensional and compressional structures.

## GEOLOGICAL FRAMEWORK

The Southern Apennine is considered an accretionary wedge (Pescatore & Slaczka 1984, Roure *et al.* 1991). It results mainly from NE-vergent thrusting of Mesozoic–Tertiary sedimentary units over the Apulian foreland (Figs. 1b and 2). According to the most recent models (Mostardini & Merlini 1988, Casero *et al.* 1988), the eastern thrust units (Lagonegro–Molise) derive from a relatively deep Mesozoic–Tertiary basinal domain originally located between two shallow-water carbonate platforms. Thrust units deriving from a western platform crop out in the western (Tyrrhenian) side of the belt (Figs. 1b and 2). Other units deriving from an eastern platform (Apulian platform) constitute a deeply buried overthrust belt detected by seismic data (Fig. 2).

A widely accepted model for the formation of an accretionary wedge is that thrusting and foredeep subsidence have progressively migrated towards the foreland. The Neogene cratonward shifting of the Apennine foredeep is well documented (Bortolotti *et al.* 1970, Casnedi *et al.* 1982, Ricchi Lucchi 1986). In the Southern Apennines, because of the progressive flexure of the Adriatic plate, the Pliocene–Quaternary terrigeneous marine deposits of the foredeep basin overlap Mesozoic–Tertiary shallow-water carbonates of the eastern platform (Fig. 2). Near the Tyrrhenian coast, the presence of Messinian clastic sediments above the car-

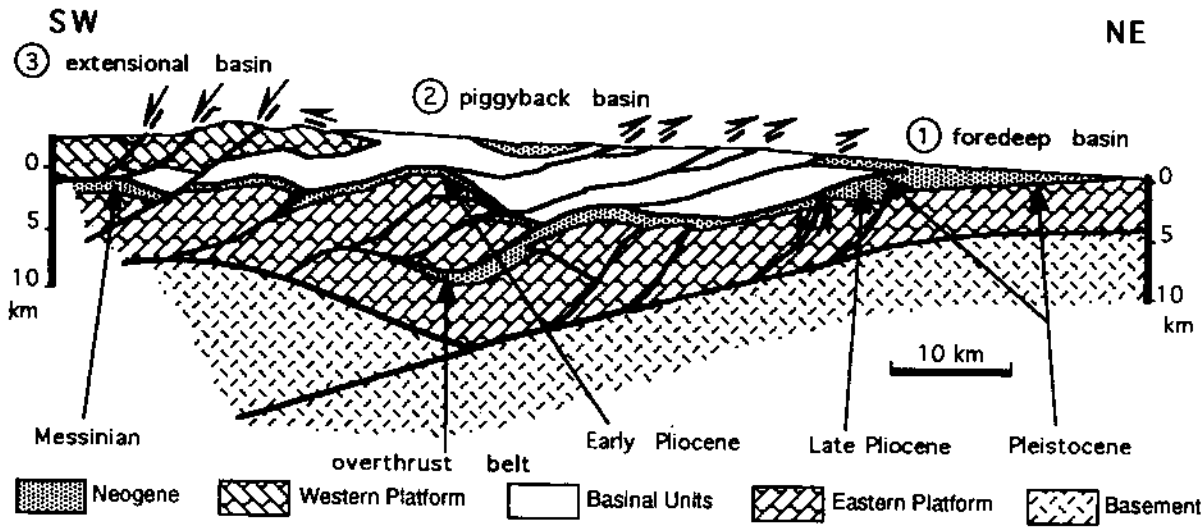


Fig. 2. Schematic cross-section of Southern Apennines (modified from Casero *et al.* 1991) showing the relationship between structural units and syn-tectonic basins (foredeep, piggyback and back-arc basins). The east–west variation in the age of the foredeep sediments shows the progressive age of the Eastern (Apulian) Platform subsidence.

bonates of the eastern platform and under the thrust sheets confirms the shifting of the subsidence (Casero *et al.* 1988) (Fig. 2).

The eastward migration of the deformation (Pescatore & Slaczka 1984) is also demonstrated by the analyses of syn-orogenic intramountain basins unconformably overlying the allochthonous units (Casero *et al.* 1988, Roure *et al.* 1991) and named piggyback basins (Ori and Friend, 1984) (Fig. 2). In particular, the ages of the Pliocene–Quaternary piggyback basins illustrate the progressive eastward shift of thrusting in the eastern platform units (Hippolyte *et al.* 1994b).

In this model of prograding deformation, supported by dating of compression in the belt and dating of flexure in the foreland, compression is considered to be the unique and permanent mode of deformation at the front of the belt. This consideration is supported by detailed palaeostress analyses in piggyback basins, showing that compression lasted for long periods and probably was even continuous on the eastern side of the belt (Hippolyte *et al.* 1994b). The extension that developed mainly on the Tyrrhenian side of the belt (Fig. 2) is hard to reconcile with this model (e.g. Ghisetti & Vezzani 1981, Moussat 1983, Malinverno & Ryan 1986, Roure *et al.* 1990). We have analysed the structure and faulting in various syn-orogenic basins to determine the place and significance of extension within the geodynamic process of accretion. In this paper, we show that extensional structures of very different ages are present on the Tyrrhenian side of the belt. The relationship with the compressional structures is determined. Three cases are observed: (1) extension pre-dating thrusting and compression; (2) extension on the Tyrrhenian side of the belt contemporaneous with thrusting and compression on the front of the belt; and (3) extension post-dating compression. These relationships are illustrated through several examples, where they are characterized in terms of stresses.

## EXTENSION PRECEDING THRUSTING

The carbonate thrust units on the western side of the belt (W.P.U. in Fig. 1b) are deformed both by extensional and compressional tectonics. Extensional structures are particularly well developed in the Matese Mountains (Figs. 1b and 3), where normal faults with offsets of several hundred metres are common (Figs. 3 and 4a). Folds, reverse faults and strike-slip faults are also present (Clermonté & Pironon 1979). All these structures are related to several states of stress including three extensional ones and three compressional and strike-slip ones.

First of all, the nature, orientation, relative chronology and stratigraphic age of each state of stress need to be discussed. A NNE–SSW extension (state of stress A in Fig. 4a) gave the best expressed deformation, with E–W trending normal faults (Fig. 3) which have large offsets (Fig. 4a). We also determined two perpendicular extension trends, NE–SW and NW–SE (Table 1, states of stress B and C) but the corresponding normal faults have much smaller offsets. A pervasive N–S to NNE–SSW compression (state of stress D in Fig. 4a) induced folding and reverse faulting. Local strike-slip and reverse motions are due to ESE–WNW and ENE–WSW compressions (states of stress E and F, respectively, Table 1).

All these faults, normal, strike-slip or reverse, affect the whole stratigraphic sequence, including the most recent deposits of the Matese unit of late Miocene age (Fig. 4a). In order to establish the chronology of these structures, we paid particular attention to geometrical relationships. For instance, when several striations are present on a single fault plane, their order of succession reveals the chronology of the relative states of stress. In the western Matese Mountains, 32 unambiguous chronologies of slickenside superposition are found. Using the chronology matrix analysis proposed by Angelier

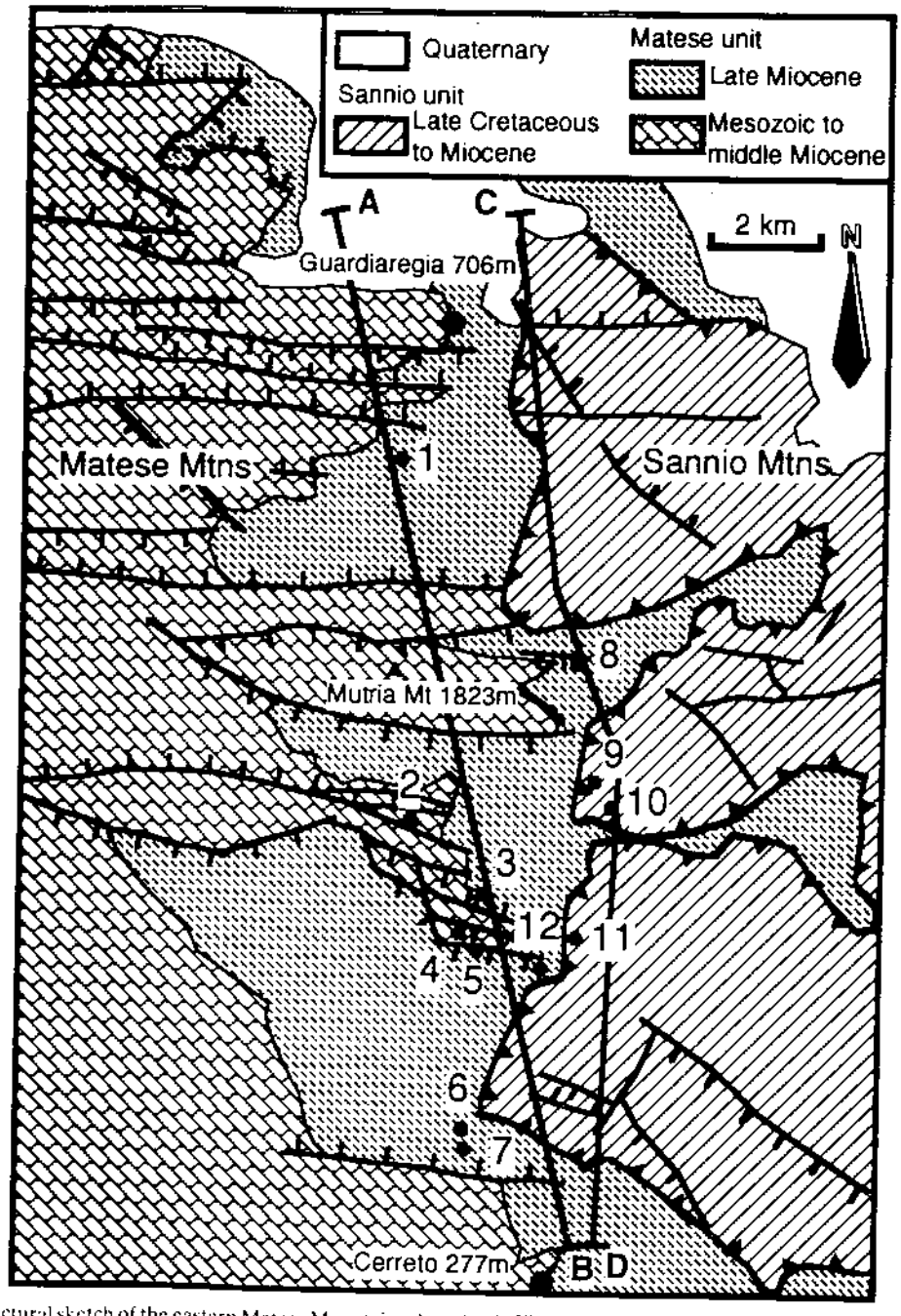


Fig. 3. Structural sketch of the eastern Matese Mountains (location in Fig. 1b). Note the differences of fracture orientations in the Sannio thrust unit and in the underlying Matese unit.

(1991), we determined the possible succession of states of stress. Among 720 possible chronologies for six states of stress, only three are consistent with all the relationships observed in the field (Fig. 5). Furthermore, for each of these three solutions, all extensional states of stress (states of stress A, B and C) pre-date compression. We conclude that, despite the apparent complexity of the palaeostress history, the widespread extensional tectonics of the Matese area certainly pre-dates the compressional tectonics.

Other criteria for chronology are found, such as cross-cutting relationships. For instance, in site 1 of Fig. 3, the normal faults of the NNE–SSW extension are offset by bedding plane faults related to folding under the NNE–SSW compression (Fig. 6a). Moreover, some of these normal faults underwent strike-slip to reverse reactivation due to the NNE–SSW compression. Both criteria indicate that normal faulting pre-dates compression. A common consequence of this chronology is that some normal faults, that have undergone tilting, now appear as nearly vertical faults or reverse faults (Figs. 4a, 6b & c).

This chronology between extension and compression is also recognized at the regional scale. The major structures of the Matese Mountains plunge to the east beneath the Sannio thrust unit (Figs. 3 and 7a) (Clermonté & Pironon 1979). The large E–W trending normal faults, which are a common feature in the Matese Mountains, do not exist in the overlying Sannio thrust sheet (Fig. 3). Furthermore, no mappable extension of

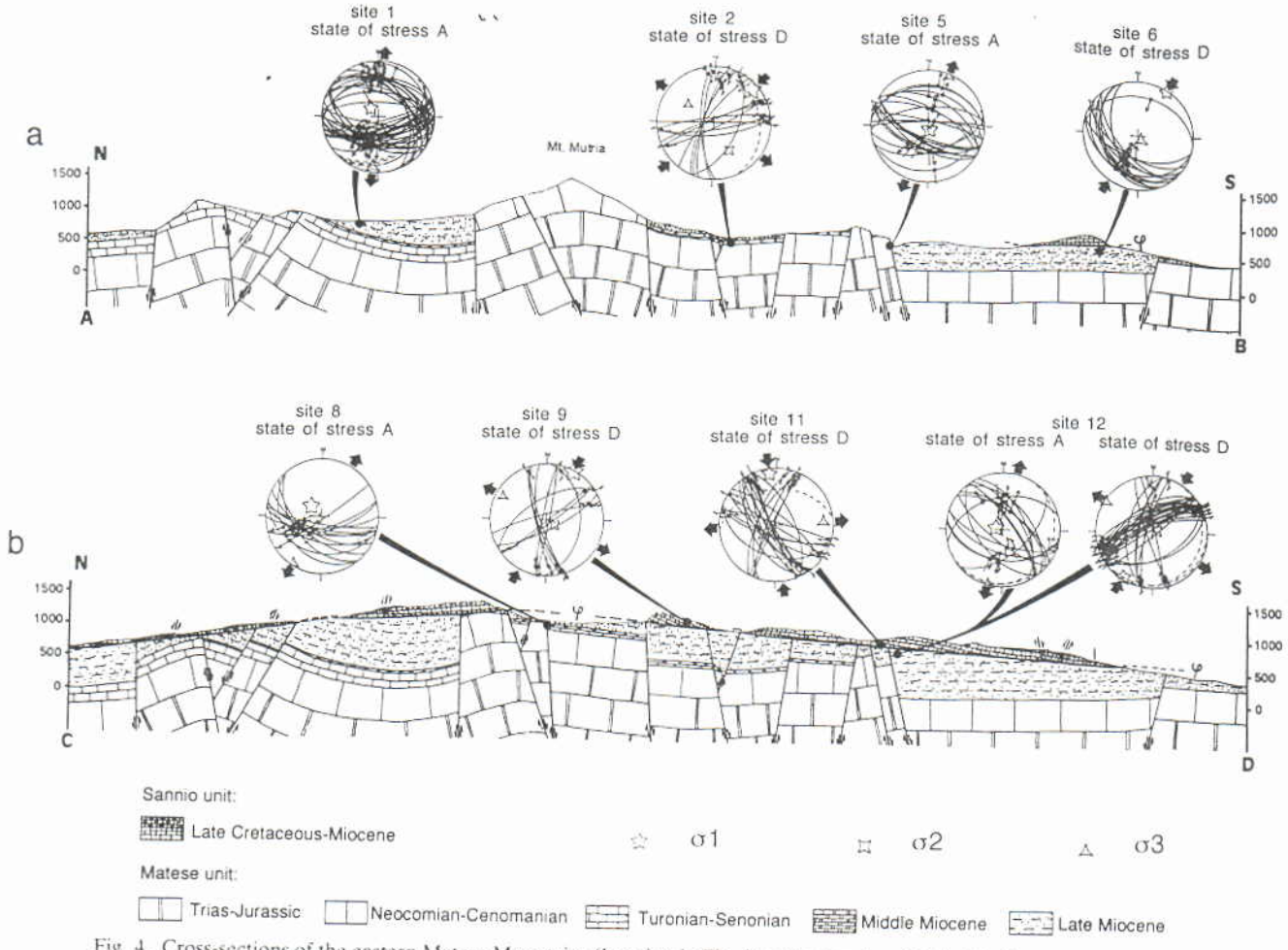


Fig. 4. Cross-sections of the eastern Matese Mountains (location in Fig. 3) and examples of Schmidt diagrams with faults and computed stress axes (see Table 1). Axes of computed palaeostress: five-branch star = $\sigma_1$, four-branch star = $\sigma_2$ and three-branch star = $\sigma_3$. In (a), normal faults with several hundred metre offsets are tilted within the folds. The major normal faults moved during NNE–SSW trending extension. In (b), the extensional structures of the Matese are sealed by the more recent Sannio back-thrust unit probably thrusted with NNE–SSW-trending compression.

these large normal faults, which have vertical separations of several hundred meters at the eastern limit of the Matese Mountains (Fig. 4a), is found in the Sannio unit. As shown in the cross-section of Fig. 4(b), the Sannio back-thrust (Fig. 3) seals the normal faulting structures of the Matese. This observation of major normal faults pre-dating major thrusts also confirms that in the Matese most of extensional deformation pre-dates compression.

For a better dating of these tectonic states of stress, we took into account the relations of the faults with the stratigraphy. Southeast of the Matese Mountains, the three compression trends (NNE–SSW, ESE–WNW and ENE–WSW) affect the Pliocene filling of piggyback basins (Fig. 1b). Northwest of the Matese Mountains (near Arpino, Fig. 1b), the ENE–WSW compression affects sediments as young as the early–middle Pleistocene. As for the Ofanto piggyback basin (Hippolyte *et al.* 1994b), these three compression trends are Pliocene–Quaternary in age, the oldest (NNE–SSW) being Pliocene or slightly older. Therefore, the normal faults predating the Pliocene–Pleistocene compression and affecting the Tortonian–Messinian flysch of the Matese Mountains, are late Miocene in age. Furthermore, the comparison between the large offsets on the E–W trending faults (several hundred metres) and the thickness variations of the late Miocene deposits (Fig. 4) suggests that this late Miocene normal faulting occurred during the deposition of the flysch sediments.

From the observation of normal faulting pre-dating compression and thrusting, we infer that the extension in the Matese Mountains cannot be considered as part of the Tyrrhenian extension that would have recently shifted into the mountain belt. This extension in the Matese is late Miocene in age, whereas the extension affecting the Tyrrhenian continental margin of the Southern Apennines is younger, mainly Pliocene–Pleistocene (Bartole *et al.* 1984).

As mentioned above, the major late Miocene extension of the Matese is very probably associated with deposition of the thick flysch formation of the same age. The western platform sedimentation comprised shallow-water carbonates since Jurassic times and changed to marls during the Serravallian, then to flysch during the late Miocene (Fig. 4). According to Casero *et al.* (1988), this change results from a rapid subsidence due to the shift of the foreland carbonate platform into a foredeep during the subduction process (Fig. 2). Effectively, the

Table 1. Palaeotress tensors computed from fault-slip data of the Matese mountains. Site localities are shown in Fig. 3. $S$ = state of stress: A = NNE–SSW-trending extension; B = NE–SW-trending extension; C = NW–SE-trending extension; D = N–S to NNE–SSW-trending compression; E = ESE–WNW-trending compression; F = ENE–WSW-trending compression. $N$ = number of faults used for tensor calculation. Stress axes: trend and plunge in degrees; $\phi = (\sigma_2 - \sigma_3)/(\sigma_1 - \sigma_3)$; Ang. = average angle between computed shear stress and observed slickenside lineation (in degrees)

| Site | Age of rocks | $S$ | $N$ | Orientation of palaeostress $\sigma_1$ | $\sigma_2$ | $\sigma_3$ | $\Phi$ | Ang. |
|---|---|---|---|---|---|---|---|---|
| 1 | Tortonian | E | 20 | 287 05 | 042 78 | 196 11 | 0.62 | 09 |
| | | F | 17 | 068 06 | 199 80 | 337 07 | 0.24 | 13 |
| | | D | 16 | 033 08 | 283 69 | 126 20 | 0.22 | 08 |
| | | B | 32 | 327 70 | 148 20 | 058 00 | 0.35 | 10 |
| | | C | 35 | 341 77 | 232 04 | 141 12 | 0.44 | 09 |
| 2 | Serravallian | A | 41 | 318 74 | 093 11 | 186 11 | 0.52 | 07 |
| 3 | Langhian | D | 14 | 047 13 | 150 43 | 304 44 | 0.18 | 10 |
| | | D | 16 | 193 14 | 311 62 | 096 24 | 0.42 | 07 |
| 4 | Cretaceous | B | 8 | 168 65 | 072 03 | 340 25 | 0.04 | 18 |
| | | F | 10 | 070 07 | 161 03 | 271 82 | 0.35 | 08 |
| 5 | Tortonian | C | 4 | 333 75 | 211 08 | 119 13 | 0.35 | 05 |
| 6 | Late Miocene | A | 21 | 161 84 | 291 04 | 021 05 | 0.46 | 08 |
| | | D | 23 | 032 03 | 302 03 | 169 86 | 0.46 | 07 |
| | | A | 7 | 286 76 | 126 13 | 035 05 | 0.34 | 12 |
| 7 | Tortonian | E | 18 | 319 11 | 127 78 | 229 02 | 0.26 | 13 |
| | | C | 10 | 023 77 | 208 13 | 298 01 | 0.42 | 13 |
| | | A | 9 | 079 73 | 304 12 | 211 12 | 0.19 | 15 |
| 8 | Cretaceous | D | 19 | 046 27 | 182 55 | 305 21 | 0.22 | 11 |
| | | A | 14 | 313 69 | 119 21 | 211 05 | 0.22 | 06 |
| 9 | Cretaceous | C | 12 | 207 81 | 053 08 | 322 04 | 0.38 | 07 |
| | | C | 10 | 333 68 | 194 17 | 099 14 | 0.45 | 11 |
| | | D | 13 | 028 02 | 127 76 | 298 14 | 0.14 | 14 |
| 10 | Cretaceous | E | 4 | 294 21 | 087 67 | 201 10 | 0.34 | 08 |
| 11 | Cretaceous | C | 13 | 006 80 | 236 06 | 145 07 | 0.70 | 06 |
| | | D | 22 | 352 10 | 234 69 | 085 18 | 0.46 | 18 |
| | | C | 19 | 168 77 | 032 09 | 300 09 | 0.37 | 09 |
| 12 | Late Miocene | B | 17 | 004 83 | 148 06 | 239 04 | 0.54 | 12 |
| | | A | 16 | 286 80 | 104 10 | 194 00 | 0.37 | 10 |
| | | C | 8 | 147 84 | 030 05 | 120 04 | 0.36 | 09 |
| | | D | 35 | 212 04 | 076 84 | 302 04 | 0.33 | 10 |

**SOLUTION 1:**

| A | Succession B | C | A | D | F | E |
|---|---|---|---|---|---|---|
| B | | 6 | | 3 | 5 | 1 |
| C | | | | 2 | 1 | 1 |
| A | | | | 1 | 2 | 2 |
| D | | | | | 5 | 2 |
| F | | | | | | 1 |
| E | | | | | | |

**SOLUTION 2:**

| | Succession B | A | C | D | F | E |
|---|---|---|---|---|---|---|
| B | | | 6 | 3 | 5 | 1 |
| A | | | | 1 | 2 | 2 |
| C | | | | 2 | 1 | 1 |
| D | | | | | 5 | 2 |
| F | | | | | | 1 |
| E | | | | | | |

**SOLUTION 3:**

| | Succession A | B | C | D | F | E |
|---|---|---|---|---|---|---|
| A | | | | 1 | 2 | 2 |
| B | | | 6 | 3 | 5 | 1 |
| C | | | | 2 | 1 | 1 |
| D | | | | | 5 | 2 |
| F | | | | | | 1 |
| E | | | | | | |

Fig. 5. Chronologies for the three possible successions of states of stress identified in the eastern Matese Mountains (method: Angelier 1991). The table indicates the number of chronological relationships observed between the state of stress in a column and the state of stress in the line (A, B, C, D, E & F, as in Table 1). For the three possible successions, all extensional states of stress (A, B & C) pre-date all compressional states of stress.

Fig. 6. Example of normal faults pre-dating compression. (a) Conjugate normal faults offset by bedding-plane faults during folding (site 1 of Fig. 3). Some normal faults have a strike-slip motion overprinting the normal motion. With the bedding plane faults, they indicate NNE–SSW-trending compression. (b) Tilted conjugate normal faults in Miocene sandstones. During folding, the bedding plane and the normal faults (event 1) have been tilted (event 2; compare with a). The site is located in the Neogene folds of the eastern Sannio Mountains (Fig. 1b); similar structures were observed in the Matese Mountains. (c) Tilted normal fault (north of site 1, Fig. 3); $S_0$ = bedding plane; C = Cretaceous limestone; M = late Miocene marls. The bedding plane dips to the southeast (left-hand side). The late Miocene marls are downfaulted relative to Cretaceous limestone. Associated with the large fault are conjugated minor faults similar with those of (b) (not visible in this photograph) which indicate that this reverse fault is a tilted normal fault.

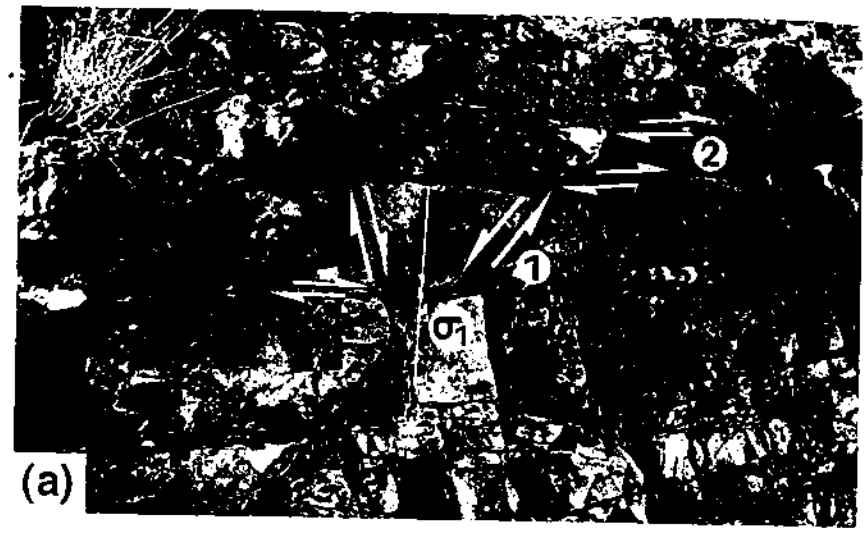
2
1
σ1
(a)

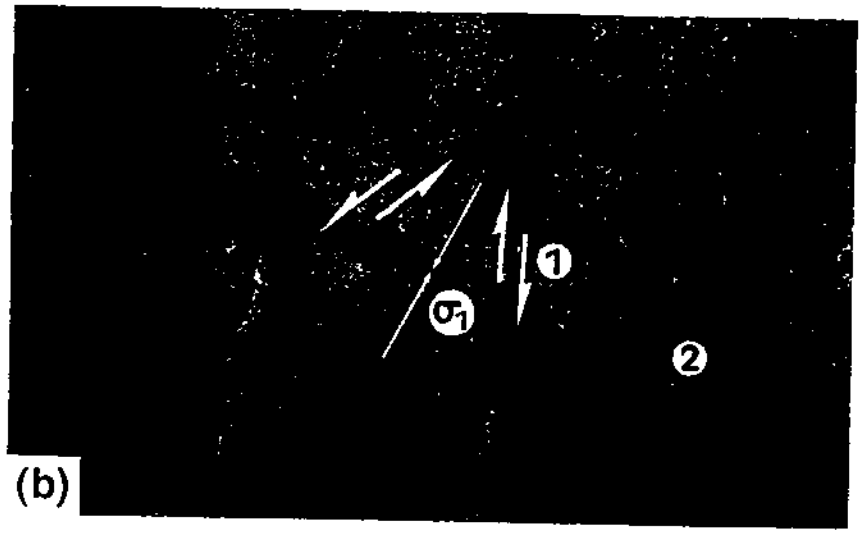
1
σ1
2
(b)


S
N
S0
C
(c)

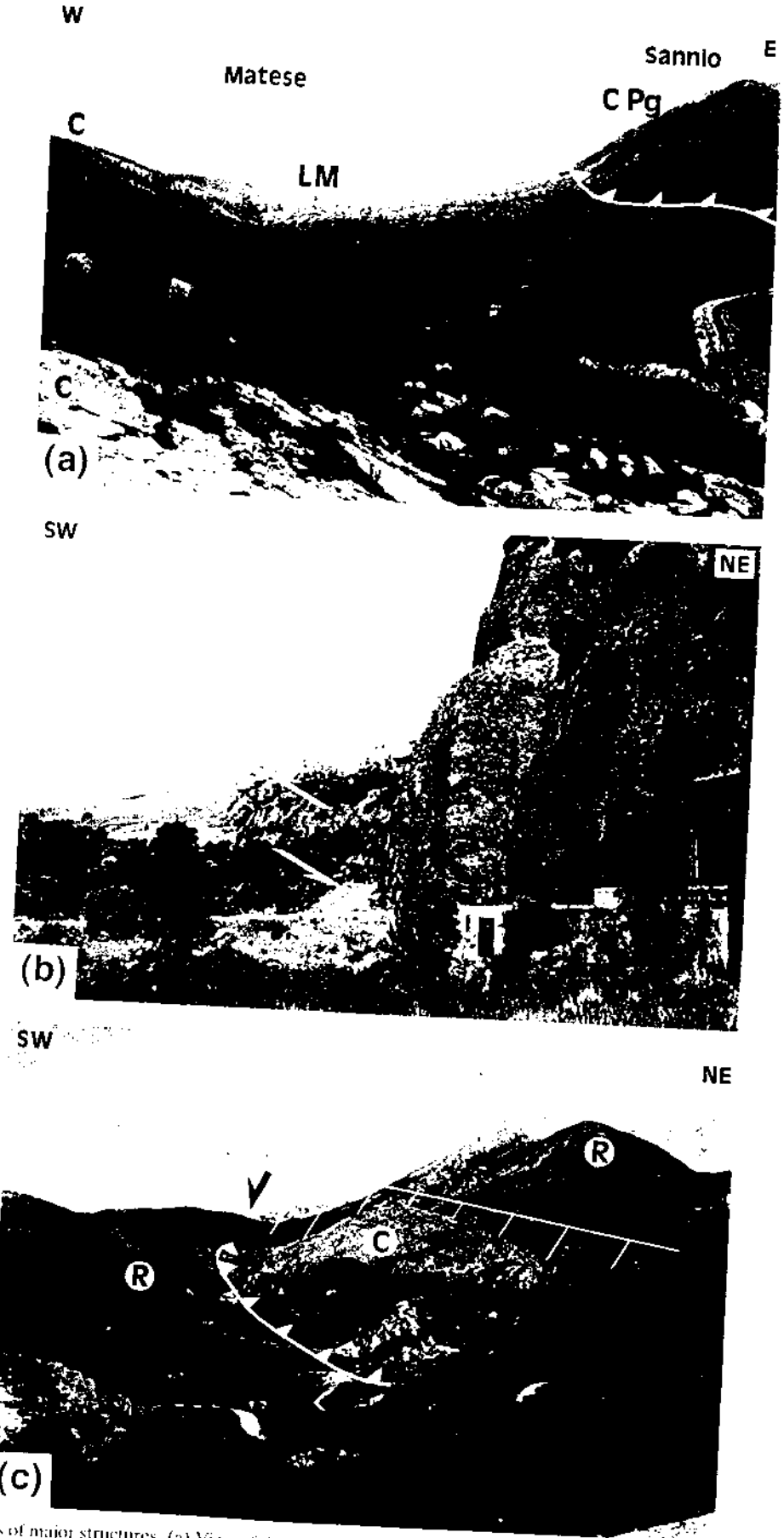


Fig. 7. Examples of major structures. (a) View of the Sannio unit overthrusting the Matese unit (close to site 9 of Fig. 3): C = Cretaceous limestone; LM = late Miocene marls (this stratigraphic unit contains olistoliths in its upper part); C, Pg = Cretaceous and Palaeogene limestone and conglomerate. The Matese Cretaceous limestone dips toward the Sannio unit. The white cliff in the Matese unit corresponds to the large normal fault south of the Mutria Mountain, scaled by the Sannio thrust unit (Figs. 3 and 4b). (b) Early Pleistocene sinistral strike-slip fault along the northern rim of the Sant'Arcangelo Basin (site 11 of Fig. 8). (c) Example of normal faulting post-dating thrust tectonics (Val D'Agri middle Pleistocene graben, located immediately West of Sant'Arcangelo Basin in Fig. 1). A klippe of Cretaceous carbonates (C, clear in the centre of photograph) belongs to the W.P.U. (Fig. 1) which is thrusted, even farther to the northeast, over radiolarites (R, dark on photograph) of the L.M.U. (Fig. 1). The thrust contact was cut by a normal fault which offsets the top of the radiolarite unit.